The Journal of Headache and Pain

RESEARCH

Open Access

Brain structural and functional abnormalities associated with acute post-traumatic headache: iron deposition and functional connectivity

Simona Nikolova[1], Catherine Chong[1,5,6], Jing Li[2], Teresa Wu[3,5], Gina Dumkrieger[1], Katherine Ross[4], Amaal Starling[1] and Todd J. Schwedt[1,5*]

Abstract

Background The purpose of this study was to interrogate brain iron accumulation in participants with acute post-traumatic headache (PTH) due to mild traumatic brain injury (mTBI), and to determine if functional connectivity is affected in areas with iron accumulation. We aimed to examine the correlations between iron accumulation and headache frequency, post-concussion symptom severity, number of mTBIs, and time since most recent TBI.

Methods Sixty participants with acute PTH and 60 age-matched healthy controls (HC) underwent 3T magnetic resonance imaging including quantitative T_2^* maps and resting-state functional connectivity imaging. Between group T_2^* differences were determined using T-tests ($p < 0.005$, cluster size threshold of 90 voxels). For regions with T_2^* differences, two analyses were conducted. First, the correlations with clinical variables including headache frequency, number of lifetime mTBIs, time since most recent mTBI, and Sport Concussion Assessment Tool (SCAT) symptom severity scale scores were investigated using linear regression. Second, the functional connectivity of these regions with the rest of the brain was examined (significance of $p < 0.05$ with family wise error correction for multiple comparisons).

Results The acute PTH group consisted of 60 participants (22 male, 38 female) with average age of 42 ± 14 years. The HC group consisted of 60 age-matched controls (17 male, 43 female, average age of 42 ± 13). PTH participants had lower T_2^* values compared to HC in the left posterior cingulate and the bilateral cuneus. Stronger functional connectivity was observed between bilateral cuneus and right cerebellar areas in PTH compared to HC. Within the PTH group, linear regression showed negative associations of T_2^* in the left posterior cingulate with SCAT symptom severity score ($p = 0.05$) and T_2^* in the left cuneus with headache frequency ($p = 0.04$).

Conclusions Iron accumulation in posterior cingulate and cuneus was observed in those with acute PTH relative to HC; stronger functional connectivity was detected between the bilateral cuneus and the right cerebellum. The correlations of decreased T_2^* (suggesting higher iron content) with headache frequency and post mTBI symptom

*Correspondence:
Todd J. Schwedt
Schwedt.Todd@mayo.edu

Full list of author information is available at the end of the article

severity suggest that the iron accumulation that results from mTBI might reflect the severity of underlying mTBI pathophysiology and associate with post-mTBI symptom severity including PTH.

Keywords T_2^*, Imaging, Post traumatic headache, Mild traumatic brain injury, Iron, Magnetic resonance imaging, Structural, Anatomical, Functional connectivity

Background

An increasing amount of evidence indicates that iron plays a detrimental role in the pathogenesis of TBI [3–6]. Iron accumulation has been identified in specific areas in the brain among patients with mild TBI (mTBI) [3–5, 7]. Since the underlying mechanisms of post-traumatic headache (PTH) following mTBI are yet to be completely defined, the purpose of this study was to investigate a potential contribution from brain iron deposition. Iron is detected with magnetic resonance imaging through the use of susceptibility weighted imaging sequences, including T_2^* sequences [8–10]. Decreased T_2^* signal has been shown to associate with increased iron accumulation [9, 11]. T_2^* changes have been found in neurological disorders such as Parkinson's Disease and have been linked to cognitive decline and aging [12–14].

Iron deposits have been reported in areas of pain processing and deep brain structures of individuals with migraine [15–20]. Iron accumulation in the periaqueductal gray matter and anterior cingulate has been shown to correlate with duration of migraine and number of migraine episodes [17–19]. Recent studies suggest that iron deposits play a role in migraine chronification [15, 16]. T_2^* changes have been observed in longitudinal studies of migraine treatment, suggesting that effective migraine treatment impacts brain iron accumulation [21]. There are fewer investigations into iron concentrations among participants with PTH. One of our prior studies has shown that PTH is associated with increased iron deposits in cortical, occipital, hippocampal and brainstem regions [22].

To interrogate acute PTH pathophysiology, this study aimed to identify brain areas with T_2^* differences in those with PTH relative to healthy controls (HC) and to determine if these areas with structural differences demonstrate altered resting-state functional connectivity. Associations between iron deposition and clinical characteristics were investigated to gain insights into relationships between abnormal brain structure with mTBI and acute PTH characteristics.

Methods

Subject enrollment

This study was approved by the Mayo Clinic and Phoenix VA Institutional Review Boards. Study participants were between 18 and 65 years of age. PTH participants were enrolled from Mayo Clinic Arizona and the Phoenix VA Health Care System and HCs were recruited through advertisements and word-of-mouth. All participants completed an informed consent process and signed informed consent forms. Data were collected over a three-year period between 2020 and 2023. Participants were diagnosed with acute PTH due to mTBI using the ICHD-3 criteria [23]. PTH participants were enrolled between the day of their injury until 59 days post mTBI. Participants completed questionnaires and structured interviews that collected data on patient demographics, current and prior mTBI characteristics, and headache characteristics [24]. Exclusion criteria for HC and PTH included gross anatomical abnormalities on brain MRI, history of severe psychiatric disorder as assessed by the principal investigator, such as but not limited to schizophrenia and bipolar disorder, history of speech disorders, pregnancy, and history of moderate or severe TBI, contraindications to MRI or history of medical condition that contraindicates research participation, chronic headache within 12 months prior to the mTBI that led to the current PTH (including PPTH, chronic migraine, medication overuse headache, new daily persistent headache, hemicrania continua, or chronic tension type headache), use of headache preventive medication within 3 months prior to screening, use of onabotulinumtoxinA in the head, neck or face in the prior 12 months, and use of opioids or barbiturates on at least 4 days per month during the 6 months before screening. HC participants were excluded if they had history of mTBI or migraine. HC participants with tension-type headaches on three or fewer days per month were not excluded.

Imaging Acquisition

Neuroimaging was performed on a 3T Siemens scanner (Siemens Magnetom Skyra, Erlangen, Germany) at Mayo Clinic Arizona. A 20-channel head and neck coil was used for all imaging. T_1-weighted images were acquired for anatomical reference using a magnetization prepared rapid image acquisition gradient echo (MPRAGE) sequence with 1 mm isotropic resolution with echo time (TE=3.03 ms), repetition time (TR=2400 ms), and flip angle (FA=8 degrees) covering $160\times256\times256$ mm^3. To obtain T_2^* maps, 12 T_2-weighted gradient echo (GRE) magnitude images were used with varying echo times (TE=2.81, 5.71, 8.06, 10.46, 12.93, 15.4, 17.86, 29.78, 42.34, 54.9, 67.46 and 80 ms). Each GRE was a stacked 2D axial image with FA of 60 degrees, TR of 3200ms, in-plane resolution of 0.94×0.94 mm, slice thickness of 4 mm and FOV of $240\times240\times132$ mm^3.

Two five-minute runs of resting state blood oxygen level dependent (BOLD) imaging with TE of 27 ms, TR of 2500 ms, FOV 64×64×64 mm^3, FA of 90 degrees, and voxel size 4×4×4 mm were collected while participants relaxed with their eyes closed. For each participant, the T_1 and T_2 imaging sequences were reviewed by a neuroradiologist, and imaging was excluded from further analyses if abnormal brain imaging findings were present.

Image Postprocessing

Data pre-processing was done using SPM12 software (Wellcome Department of Cognitive Neurology, Institute of Neurology, London, UK) in conjunction with MATLAB version R2019b (Mathworks, Natick, MA, USA). T_2^* maps were smoothed with a 6 mm kernel and resampled to match the T_1-weighted images. The T_1-weighted images were used to normalize to Montreal Neurological Institute (MNI) space along with the co-registered T_2^* to yield 1 mm isotropic resolution maps. A 4 mm dilated mask was used to remove cerebrospinal fluid (CSF) contamination.

Functional images were motion corrected, realigned to the first image of the set, coregistered to the anatomical T_1-weighted image, realigned to the average MNI template, and smoothed using an 8 mm FWHM Gaussian kernel using SPM12. Further post processing in AFNI 3dTproject included band pass filtering (0.01–0.1 Hz) after removal of nuisance signals from framewise displacement, cerebrospinal fluid signal, and linear drift. The first five frames were excluded to allow the signal to reach steady state. Frames with excess of 2 mm motion were also removed from the analysis. Region of interest to brain correlation maps were calculated using MATLAB. Regions of significant T_2^* difference between PTH and HC were used to select the regions of interest for the functional connectivity analysis. Left and right hemisphere clusters were interrogated separately. The Pearson correlation coefficients were calculated between the region of interest and the rest of the brain using in-house software written in MATLAB. The correlation maps were Fisher transformed to Z-scores for group comparisons.

Statistical analysis

The number of participants (N=60 per group) was not chosen a-priori based on a power analysis. All available data was used for these analyses. T_2^* differences between 60 PTH participants and 60 age-matched HC were evaluated in MNI space using a t-test within SPM12 (https://www.fil.ion.ucl.ac.uk/spm/software/spm12/) compensating for age and sex. Cluster analysis was performed in SPM 12 using uncorrected $p<0.005$ and volume threshold of 90 mm^3 (90 voxels) to interrogate T_2^* differences in PTH compared to HC. Cluster labelling was assisted with automated anatomical atlas ROI_MNI_V7.

The average T_2^* values from regions with significant T_2^* differences were included in a linear model to assess association with clinical variables within the PTH group. The clinical variables examined were number of lifetime mTBIs, time since most recent mTBI, the Sport Concussion Assessment Tool (SCAT) symptom severity checklist score, and headache frequency. Headache frequency was calculated as the percentage of days with headache since mTBI.

The regions with significant T_2^* differences between PTH and HC were used as seeds for a for full brain resting state functional connectivity correlation analysis. A full factorial analysis was conducted in SPM12 with two factors: group factor with two levels for PTH and HC and region of interest factor with the number of levels equal to the number of regions of interest used, as well as covariates to compensate for age and sex. Group differences for each region of interest were examined with a F-statistic with post hoc t-tests used to assess direction of the effect. Significance for group differences was set to $p<0.05$ with family wise error correction for multiple comparisons.

Results

A total of 120 participants were included in the analysis. Participant demographics, headache characteristics, and mTBI characteristics are shown in Table 1. The acute PTH group consisted of 60 participants (22 male, 38 female) with average age of 42 years (SD=14, range from 19 to 70). The HC group consisted of 60 age-matched controls (17 male, 43 female) with an average age of 42 (SD=13, range from 21 to 71). Age matching (PTH-HC) had an average difference of 0.1 years (SD=2, range −3.6 to 5.3 years).

The symptoms included in the ICHD-3 diagnostic criteria for primary headaches were used to classify the PTH phenotypes: 35 participants with PTH had migraine-like headache phenotypes, 8 had probable migraine-like phenotypes, 14 had tension-type-like headache phenotypes, 1 had probable tension type-like headache phenotype, and 2 participants' PTH phenotypes were not classifiable.

45% of all PTH participants suffered a mTBI due to a fall, 30% due to motor vehicle accident, 12% due to a fight, 7% hit against object, 5% due to a sport injury, and 2% hit by object. 46% of PTH participants had one lifetime mTBI, 17% had two mTBIs, 16% had three, 5% had four, and 16% had 5 or more lifetime TBIs. 53% of PTH participants had headache before their most recent TBI. The mTBI was accompanied by loss of consciousness in 36% of PTH participants, alteration of consciousness in 53%, and amnesia in 40%. For all participants, the number of reported days between mTBI and imaging ranged from 4 to 50 days with an average of 25 days (SD=15 days). Twenty-seven participants had PTH onset immediately

Table 1 Participant demographics and post traumatic headache clinical variables and phenotypes. Time since mTBI is the number of days between the date of mTBI and the baseline research visit. Headache frequency is reported as the percent number of days since mTBI with headache. Average headache intensity is reported on a scale of 0 = no pain to 10 = maximum pain. Time from mTBI to PTH is the number of hours between the brain injury and headache onset. Values reported as mean ± standard deviation. Abbreviations: mTBI = mild traumatic brain injury, PTH = post traumatic headache, HC = healthy controls, SCAT = Sport Concussion Assessment Tool

	PTH (*n* = 60)	HC (*n* = 60)
Age (years)	41.7 ± 13.7	41.5 ± 13.4
Sex (male/female)	22/38	17/43
Headache frequency (%)	81 ± 28	N/A
Average headache intensity	4.6 ± 1.8	N/A
Number of lifetime mTBIs	2.4 ± 1.9	N/A
Time since most recent mTBI (days)	25 ± 15	N/A
SCAT symptom checklist score	29 ± 23	N/A
SCAT # post TBI symptoms	12 ± 7	N/A
Beck Depression Inventory score	11 ± 8	N/A
TRAIT Anxiety Inventory score	38 ± 12	N/A
STATE Anxiety Inventory score	35 ± 12	N/A
Time from mTBI to PTH (hours)	17 ± 47	N/A
PTH Phenotypes		
Migraine	35	N/A
Probable migraine	8	N/A
Tension type	14	N/A
Probable Tension type	1	N/A
Not Classifiable	2	N/A

following injury, 23 had PTH starting within one day of the mTBI, and ten had PTH onset of >1 day post mTBI but prior to 7 days. PTH participants had headaches on an average of 81% of the days since their TBI (SD = 28% with a range from 7 to 100%). Fifty-five percent of PTH participants had continuous headaches.

T_2^* Imaging results

No increases of T_2^* were detected in PTH participants compared to healthy controls, whereas lower T_2^* values (suggesting increased iron) were observed in the left posterior cingulate and bilateral cuneus as shown in Fig. 1. Since the cuneus results were bilateral, the left and right sides were investigated separately in a secondary analysis to account for laterality.

T_2^* Linear regression of Headache and mTBI characteristics

For those regions that had significant T_2^* differences between PTH and HC, significant negative associations were found between SCAT symptom severity score and left posterior cingulate ($p = 0.05$) and between left cuneus and headache frequency ($p = 0.04$).

Functional Connectivity Differences in Brain Regions with T_2^* decreases

In PTH participants, the regions with decreased T_2^* in PTH compared to HC, (the posterior cingulate cortex and cuneus) were investigated for differences in resting state functional connectivity. Significantly stronger functional connectivity was observed between the right cuneus with right cerebellum and the left cuneus with right cerebellum amongst those with PTH compared to HC.

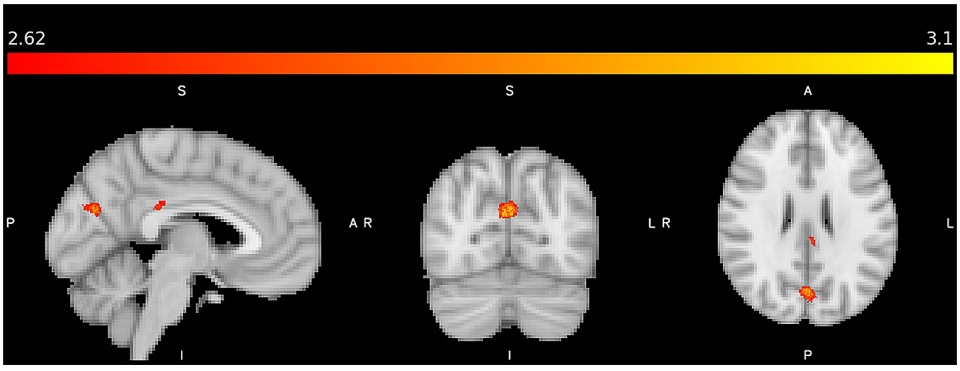

MNI			Region	Number of Voxels	Peak T-stat
x	y	z			
3	-73	25	Bilateral Cuneus	751	3.1
-3	-34	27	Posterior Cingulate Left	92	2.8

Fig. 1 Whole brain analysis of cluster results of T_2^* reduction in participants with PTH compared to age-matched HC. 3D T-statistic of T_2^* decreases in PTH participants compared to HC are shown in standardized MNI space. The two clusters surviving uncorrected $p < 0.005$ with cluster threshold of 90 mm^3 (90 voxels) are the left posterior cingulate and the bilateral cuneus. The coordinates (x, y, z) in MNI space of the cluster centers, cluster volume and the corresponding anatomical regions are shown. maximum T-statistic at the cluster center is provided

Discussion

Although the specific mechanisms associated with iron accumulation amongst those with PTH are not well-defined, possibilities include overproduction of transferrin, increased density of transferrin receptors [25], free radical cell damage, and release of iron as a result of neuronal degeneration [5, 17, 20]. It has previously been shown that iron deposition may serve as a biomarker for migraine and for duration and frequency of migraine attacks [17–19]. The effect of iron deposition in PTH following mTBI hasn't been widely investigated, but the findings from our study suggest that iron deposition might serve as a biomarker for PTH frequency. In a previous study, we observed T_2^* decreases associated with iron accumulation in twenty PTH participants compared to age matched HCs [22]. Nineteen of the twenty above-mentioned PTH participants were included in the current study, along with seventeen of the HCs. The current, larger study reports regions with T_2^* decreases consistent with previous findings [22] with more conservative thresholds used for determining significance. The current study found decreased T_2^* in the bilateral cuneus and left posterior cingulate. The cuneus is involved in visual processing, as well as having roles in working memory and cognitive control. The posterior cingulate, along with precuneus, angular gyrus and medial prefrontal cortex is a core region of the default mode network (DMN) [26–30]. Our results suggest that brain iron accumulation serves as a biomarker of PTH and mTBI burden and might provide insights into mechanisms underlying PTH and other symptoms following mTBI.

Our results suggest that T_2^* decreases may play a role in the disruption of cerebellar functional networks, previously shown in PTH after mTBI, and consistent with the hypothesis of hypersensitivity to pain and disruption of cognitive control networks [31]. Specifically, we saw increased functional connectivity from the bilateral cuneus to the cerebellum. We speculate that altered structure of the cuneus and its connectivity with the cerebellum could be associated with abnormal eye movements that often occur following mTBI, such as abnormalities in saccades, smooth pursuit, and vergence [32–34]. Unfortunately, we did not measure oculomotor dysfunction in our study.

Prior studies have demonstrated atypical structure and connectivity of DMN regions amongst those with mTBI and amongst those with PTH [31, 35, 36]. In our study, abnormal T_2^* was identified in the posterior cingulate, an important hub of the DMN. Niu et al. reported disruption in the connectivity between the DMN with the periaqueductal gray amongst those with acute PTH due to mTBI which could signify impaired pain modulation following mTBI and which was a strong predictor of PTH persistence at three months post injury [31, 35].

Zhou et al. showed reduced connectivity in the posterior cingulate and parietal regions and increased frontal connectivity in the medial prefrontal cortex in patients with mTBI relative to HC [36]. Zhou et al. also showed that the posterior connectivity correlated positively with neurocognitive dysfunction while the frontal connectivity was negatively correlated to post-traumatic symptoms such as symptoms of postconcussion syndrome. In this study, we did not interrogate functional connectivity correlations to headache severity, but we did show that headache severity correlated negatively with iron burden in the left posterior cingulate and with headache frequency in the left cuneus.

Iron accumulation in the two regions found in this study correlated with measures of headache frequency and post-mTBI symptom severity. We found negative associations of headache frequency with T_2^* in the left cuneus, one region previously identified to associate with headache frequency [19, 37, 38]. Negative association between headache frequency and decrease of gray matter volume in the cuneus was reported by Neeb et al. [38] in migraine groups compared to HCs. This finding suggests a link between pain and brain plasticity, independent of injury. The negative associations with headache frequency suggest that there may be an accumulation of iron due to recurrent headaches.

Limitations

T_2^* decrease is assumed to relate to iron accumulation, but that decrease may be due to hemorrhage, venous blood, calcification, or changes in tissue water concentration. Future work will evaluate these contrast contributions further using phase information from quantitative susceptibility imaging.

In this study, regions with T_2^* decreases consistently showed cerebellar connectivity disruption yet no T_2^* differences in the cerebellum are reported. The field of view of our T_2^* sequence consistently cropped the cerebellum and data from this region could not be reported. Future studies should expand the field of view to contain the cerebellum.

The exploratory nature of this study created numerous statistical comparisons between groups, and within group associations. In line with other exploratory whole brain studies, no corrections for multiple comparisons were made for the primary analysis to identify regions with T_2^* decreases in PTH [39]. Type I errors were mitigated through a cluster forming threshold of 90 voxels for all reported significant clusters. A correction for multiple comparisons was applied to the secondary full brain analysis for connectivity changes.

In this analysis, 32 participants had migraine prior to their mTBI. For these participants, it is not possible

to know if the imaging findings are related to migraine, PTH, or both (which is probably most likely).

The temporal dynamics of iron accumulation after mTBI has not been thoroughly investigated and is not well understood. Time since mTBI was included in the multiple linear regression analysis in the current study when investigating the effect of headache characteristics, but it is possible that non-linear models would be more appropriate.

Conclusions

Decreased T_2^* values, suggestive of increased iron accumulation, were found in the left posterior cingulate cortex and bilateral cuneus amongst those with acute PTH attributed to mTBI compared to HC. Stronger functional connectivity was observed between the bilateral cuneus and the right cerebellum. In the regions with decreased T_2^* in PTH compared to HC headache frequency and SCAT symptom severity scores correlated with iron accumulation, suggesting that the presence of iron is associated with greater mTBI and PTH burden.

Abbreviations

HC	Healthy Control
PTH	Post traumatic headache
mTBI	mild traumatic brain injury
DMN	default mode network
SCAT	sport concussion assessment tool
MPRAGE	magnetization prepared rapid image acquisition gradient echo
GRE	Gradient echo
BOLD	Blood-oxygen-level-dependent
GLM	general linear model
MNI	Montreal Neurological Institute
ROI	region of interest

Acknowledgements

The authors would like to thank the research participants for their involvement in this study.

Author contributions

All co-authors have thoroughly reviewed and assisted in the editing of this manuscript. S.N was involved in data analysis, writing the manuscript. C.C contributed to access to patients, concept design as well as manuscript editing. J.L and T.W helped with manuscript preparation and editing. G.D assisted with manuscript editing. A.S and K.R helped with manuscript editing. T.S provided access to patients, concept design and assisted with manuscript writing and editing. All co-authors agree with the content and verify that it reflects sound research methodology.

Funding

This study was funded by the United States Department of Defense, Award Number W81XWH-19-1-0534 and the National Institutes of Health, National Institute of Neurological Disorders and Stroke, Award Number 1R61NS113315-01.

Data availability

Deidentified data from this study can be made available upon request following Mayo Clinic sharing standards. Analytic code used to conduct the statistical analyses presented in this study are freely available in a public repository identified in the manuscript (SPM12). The datasets used and/or analyzed during the current study are available from the corresponding author on reasonable request.

Declarations

Ethics approval and consent to participate

This study was approved by the Mayo Clinic and Phoenix VA Institutional Review Boards.

Consent for publication

All participants completed an informed consent process and signed informed consent forms.

Competing interests

Within the prior 24 months, TJS has consulted for AbbVie, Amgen, Collegium, Eli Lilly, Linpharma, Lundbeck, Satsuma, Scilex, Theranica. He has received royalties from Up to Date and has held stock options in Aural Analytics and Nocira. He has received research grant support from American Heart Association, Amgen, Henry Jackson Foundation, National Institutes of Health, Patient Centered Outcomes Research Institute, Pfizer, Spark Neuro, United States Department of Defense. He serves on the editorial boards of Cephalalgia, Cephalalgia Reports, and the Journal of Headache and Pain. J.L and C.C have received NIH grants for support for research or education. C.C and G.D have received Amgen grant support for research. T.W serves as editor in chief of the Journal of Alzheimer's disease. A.S has received consulting fees from AbbVie, Allergan, Axsome Therapeutics, eNeura, Everyday Health, Lundbeck, Med-IQ, Medscape, Miller Medical, Satsuma, and WebMD. S.N and K.R have nothing to disclose.

Author details

[1]Department of Neurology, Mayo Clinic, 5777 East Mayo Blvd Phoenix, Phoenix, AZ 85054, USA
[2]School of Industrial and Systems Engineering, Georgia Tech, Georgia, GA, USA
[3]School of Computing, Informatics, Decision Systems Engineering, Arizona State University, Tempe, AZ, USA
[4]Phoenix VA Health Care System, Phoenix, AZ, USA
[5]ASU-Mayo Center for Innovative Imaging, Tempe, AZ, USA
[6]Department of Physiology and Biomedical Engineering, Mayo Clinic, Phoenix, AZ, USA

Received: 25 March 2024 / Accepted: 21 May 2024
Published online: 28 May 2024

References

1. Cassidy JD, Carroll LJ, Peloso PM et al Incidence, risk factors and prevention of mild traumatic brain injury: results of the WHO Collaborating Centre Task Force on mild traumatic brain Injury. J Rehabil Med 2004 Feb (43 Suppl):28–60
2. Dewan MC, Rattani A, Gupta S et al (2018 Apr) Estimating the global incidence of traumatic brain injury. J Neurosurg 1:1–18
3. Lu L, Cao H, Wei X, Li Y, Li W (2015) Iron Deposition is positively related to cognitive impairment in patients with chronic mild traumatic brain Injury: Assessment with susceptibility weighted imaging. Biomed Res Int 2015:470676
4. Raz E, Jensen JH, Ge Y et al (2011 Nov-Dec) Brain iron quantification in mild traumatic brain injury: a magnetic field correlation study. AJNR Am J Neuroradiol 32(10):1851–1856
5. Nisenbaum EJ, Novikov DS, Lui YW (2014) The presence and role of iron in mild traumatic brain injury: an imaging perspective. J Neurotrauma 31(4):301–307
6. Daglas M, Adlard PA (2018) The involvement of Iron in Traumatic Brain Injury and neurodegenerative disease. Front Neurosci 12:981
7. Lu L, Li F, Wang P, Chen H, Chen YC, Yin X (2020) Altered hypothalamic functional connectivity in post-traumatic headache after mild traumatic brain injury. J Headache Pain 21(1):93
8. Gossuin Y, Burtea C, Monseux A et al (2004) Ferritin-induced relaxation in tissues: an in vitro study. J Magn Reson Imaging 20(4):690–696
9. Gossuin Y, Muller RN, Gillis P (2004) Relaxation induced by ferritin: a better understanding for an improved MRI iron quantification. NMR Biomed 17(7):427–432
10. Schenck JF (1995) Imaging of brain iron by magnetic resonance: T2 relaxation at different field strengths. J Neurol Sci. 134 Suppl:10 – 8.

11. Yao B, Li TQ, Gelderen P, Shmueli K, de Zwart JA, Duyn JH (2009) Susceptibility contrast in high field MRI of human brain as a function of tissue iron content. NeuroImage 44(4):1259–1266
12. Ulla M, Bonny JM, Ouchchane L, Rieu I, Claise B, Durif F (2013) Is R2* a new MRI biomarker for the progression of Parkinson's disease? A longitudinal follow-up. PLoS ONE 8(3):e57904
13. Daugherty AM, Raz N (2015) Appraising the role of Iron in Brain Aging and Cognition: promises and limitations of MRI methods. Neuropsychol Rev 25(3):272–287
14. Daugherty AM, Haacke EM, Raz N (2015) Striatal iron content predicts its shrinkage and changes in verbal working memory after two years in healthy adults. J Neurosci 35(17):6731–6743
15. Chen Z, Dai W, Chen X, Liu M, Ma L, Yu S (2021 Jan-Dec) Voxel-based quantitative susceptibility mapping revealed increased cerebral iron over the whole brain in chronic migraine. Mol Pain 17:17448069211020894
16. Dominguez Vivero C, Leira Y, Saavedra Pineiro M et al (2020) Iron deposits in Periaqueductal Gray Matter Are Associated with poor response to OnabotulinumtoxinA in chronic migraine. Toxins (Basel). 12(8)
17. Kruit MC, Launer LJ, Overbosch J, van Buchem MA, Ferrari MD (2009) Iron accumulation in deep brain nuclei in migraine: a population-based magnetic resonance imaging study. Cephalalgia 29(3):351–359
18. Palm-Meinders IH, Koppen H, Terwindt GM et al (2017) Iron in deep brain nuclei in migraine? CAMERA follow-up MRI findings. Cephalalgia 37(8):795–800
19. Tepper SJ, Lowe MJ, Beall E et al (2012) Iron deposition in pain-regulatory nuclei in episodic migraine and chronic daily headache by MRI. Headache 52(2):236–243
20. Welch KM, Nagesh V, Aurora SK, Gelman N (2001 Jul-Aug) Periaqueductal gray matter dysfunction in migraine: cause or the burden of illness? Headache. 41(7):629–637
21. Nikolova S, Chong CD, Dumkrieger GM, Li J, Wu T, Schwedt TJ (2023) Longitudinal differences in iron deposition in periaqueductal gray matter and anterior cingulate cortex are associated with response to erenumab in migraine. Cephalalgia 43(2):3331024221144783
22. Nikolova S, Schwedt TJ, Li J et al (2021 Oct) T2* reduction in patients with acute post-traumatic headache. Cephalalgia 13:3331024211048509
23. Headache Classification Committee of the International Headache Society (IHS) The International Classification of Headache Disorders, 3rd edition. Cephalalgia (2018);38(1):1-211
24. Corrigan JD, Bogner J (2007 Nov-Dec) Initial reliability and validity of the Ohio State University TBI Identification Method. J Head Trauma Rehabil 22(6):318–329
25. Gomez-Flores R, Weber RJ (1999) Inhibition of interleukin-2 production and downregulation of IL-2 and transferrin receptors on rat splenic lymphocytes following PAG morphine administration: a role in natural killer and T cell suppression. J Interferon Cytokine Res 19(6):625–630
26. Utevsky AV, Smith DV, Huettel SA (2014) Precuneus is a functional core of the default-mode network. J Neurosci 34(3):932–940
27. Leech R, Kamourieh S, Beckmann CF, Sharp DJ (2011) Fractionating the default mode network: distinct contributions of the ventral and dorsal posterior cingulate cortex to cognitive control. J Neurosci 31(9):3217–3224
28. Maddock RJ, Garrett AS, Buonocore MH (2003) Posterior cingulate cortex activation by emotional words: fMRI evidence from a valence decision task. Hum Brain Mapp 18(1):30–41
29. Maddock RJ, Garrett AS, Buonocore MH (2001) Remembering familiar people: the posterior cingulate cortex and autobiographical memory retrieval. Neuroscience 104(3):667–676
30. Bluhm RL, Clark CR, McFarlane AC, Moores KA, Shaw ME, Lanius RA (2011) Default network connectivity during a working memory task. Hum Brain Mapp 32(7):1029–1035
31. Li F, Lu L, Shang S et al (2021) Altered static and dynamic functional network connectivity in post-traumatic headache. J Headache Pain 22(1):137
32. McDonald MA, Holdsworth SJ, Danesh-Meyer HV (2022) Eye movements in mild traumatic brain Injury: ocular biomarkers. J Eye Mov Res. 15(2)
33. O'Driscoll GA, Wolff AL, Benkelfat C, Florencio PS, Lal S, Evans AC (2000) Functional neuroanatomy of smooth pursuit and predictive saccades. NeuroReport 11(6):1335–1340
34. Rockswold SB, Burton PC, Chang A et al (2019) Functional Magnetic Resonance Imaging and oculomotor dysfunction in mild traumatic brain Injury. J Neurotrauma 36(7):1099–1105
35. Niu X, Bai L, Sun Y et al (2019) Disruption of periaqueductal grey-default mode network functional connectivity predicts persistent post-traumatic headache in mild traumatic brain injury. J Neurol Neurosurg Psychiatry 90(3):326–332
36. Zhou Y, Milham MP, Lui YW et al (2012) Default-mode network disruption in mild traumatic brain injury. Radiology 265(3):882–892
37. Ashina H, Iljazi A, Al-Khazali HM et al (2020) Persistent post-traumatic headache attributed to mild traumatic brain injury: deep phenotyping and treatment patterns. Cephalalgia 40(6):554–564
38. Neeb L, Bastian K, Villringer K, Israel H, Reuter U, Fiebach JB (2017) Structural Gray Matter alterations in chronic migraine: implications for a Progressive Disease? Headache 57(3):400–416
39. Perneger TV (1998) What's wrong with Bonferroni adjustments. BMJ 316(7139):1236–1238

Publisher's Note